

Effect of a magnetic field on the quasiparticle recombination in superconductors

Xiaoxiang Xi,^{1,2} J. Hwang,^{1,3} C. Martin,¹ D. H. Reitze,¹ C. J. Stanton,¹ D. B. Tanner,¹ and G. L. Carr²

¹*Department of Physics, University of Florida, Gainesville, Florida 32611, USA*

²*Photon Sciences, Brookhaven National Laboratory, Upton, New York 11973, USA*

³*Department of Physics, Sungkyunkwan University, Suwon, Gyeonggi-do 440-746, Republic of Korea*

(Received 21 November 2012; revised manuscript received 1 April 2013; published 5 April 2013)

Quasiparticle recombination in a superconductor with an *s*-wave gap is typically dominated by a phonon bottleneck effect. We have studied how a magnetic field changes this recombination process in metallic thin-film superconductors, finding that the quasiparticle recombination process is significantly slowed as the field increases. The magnetic field disrupts the time-reversal symmetry of the pairs, giving them a finite lifetime and decreasing the energy gap. The field could also polarize the quasiparticle spins, producing different populations of spin-up and spin-down quasiparticles. Both processes favor slower recombination; in our materials we conclude that strong spin-orbit scattering reduces the spin polarization, leaving the field-induced gap reduction as the dominant effect and accounting quantitatively for the observed recombination rate reduction.

DOI: [10.1103/PhysRevB.87.140502](https://doi.org/10.1103/PhysRevB.87.140502)

PACS number(s): 74.40.Gh, 74.25.Ha, 74.70.Ad, 78.47.D–

An excitation from the superconducting condensate requires finite energy (the energy gap 2Δ) and produces two quasiparticles. A quasiparticle excited to very high energy (compared to Δ) quickly decays via a number of fast scattering processes to near the gap edge, where it recombines with a partner to form a Cooper pair. The pair's binding energy is emitted mainly as 2Δ phonons.^{1–3} The recombination process is delayed by a phonon bottleneck: Each recombination-generated phonon can break another Cooper pair, causing energy to be trapped in a coupled system of 2Δ phonons and excess gap-edge quasiparticles.^{4–6} Quasiparticle recombination has been widely studied in both metallic superconductors, to investigate the nonequilibrium processes in the many-body BCS system,^{7–10} and high-temperature superconductors, to gain new insight into the pairing mechanism.^{11–14} Theories of the recombination process considered the reaction kinetics and interactions of quasiparticles and phonons,^{15,16} while experiments obtained the dependence of the quasiparticle lifetime on temperature, film thickness, and excitation strength.^{17,18}

A magnetic field is known to couple to the electron orbital motion and to align the spin; both effects weaken superconductivity.¹⁹ The consequence of magnetic field on the quasiparticle recombination²⁰ has not been examined in detail by optical pump-probe methods. This question has been largely neglected in recent studies of charge imbalance²¹ and spin-polarized quasiparticle transport^{22,23} in a magnetic field. It is also relevant to the transport study of nonequilibrium charge and energy relaxation in superconductors,^{24,25} because supercurrents and magnetic fields play equivalent roles in terms of pair breaking. We observed that the field significantly slows the quasiparticle recombination in conventional metallic thin-film superconductors. While we observe this for all field orientations, we focus here on the results for a field applied parallel to the thin-film surface, minimizing the influence of vortices. Our results surprised us; our hypothesis was that (for perpendicular fields) the normal cores of vortices in the superconductor would provide an additional channel for phonon escape, and speed up the recombination.

We use a time-resolved laser-pump synchrotron-probe spectroscopic technique to study the quasiparticle recombina-

tion dynamics in conventional metallic superconducting thin films, under applied magnetic field. Samples studied include a 10 nm thick Nb_{0.5}Ti_{0.5}N film on a crystal quartz substrate and a 70 nm thick NbN film on a MgO substrate. These substrates are essentially transparent in the far-infrared spectral range. The films were grown by reactive magnetron sputtering, using a NbTi cathode in Ar/N₂ gas for Nb_{0.5}Ti_{0.5}N and a Nb cathode in N₂ gas for NbN. The two films have critical temperatures of 10.2 K and 12.8 K, and a zero-temperature, zero-field energy gap 2Δ of 3.2 meV and 4.5 meV, respectively. Four-probe resistivity measurements with magnetic field parallel to the films determined their upper critical field to be greater than 20 T at $T \leq 3$ K.

The samples were mounted in a ⁴He Oxford cryostat equipped with a 10 T superconducting magnet, and probed by far-infrared radiation produced in a bending magnet at beamline U4IR of the National Synchrotron Light Source, Brookhaven National Laboratory. The experiment, illustrated in Fig. 1, exploits the fact that the synchrotron radiation is emitted in ~ 300 ps long pulses (governed by the electron bunch structure in the storage ring). We applied mode-locked near-infrared Ti:sapphire laser pulses (~ 2 ps in duration and ~ 1.5 eV in photon energy) as the source for photoexcitation. The synchrotron probe beam measures the photoinduced optical properties due to the excess quasiparticles as a function of time delay relative to the arrival of the pump beam. The synchrotron pulse has a Gaussian profile with a FWHM of ~ 300 ps, determining the time resolution of the experiment. At selected delay times t , we measure the spectrally integrated photoinduced transmission $S(t) \equiv -\Delta T(t)$ over the spectral range spanning the superconductor's energy gap (~ 3 meV). The spectral shape is determined primarily by the optical components carrying the beam, and the detector.

If the laser were turned on and off to measure the photoinduced response, there would be a temperature modulation as well as the photoexcited quasiparticle modulation. To reduce these thermal effects we dither the laser pulse back and forth by a few tens of picoseconds at each delay setting, keeping the incident laser power constant. The dither is achieved by phase-modulating the laser pulse using the internal oscillator of

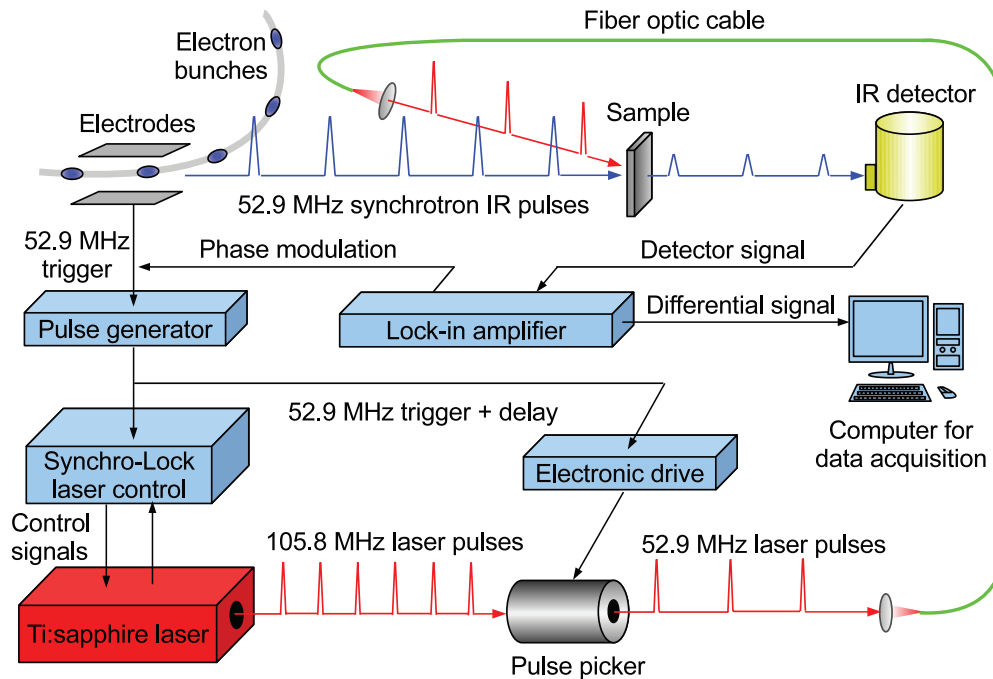


FIG. 1. (Color online) Experimental setup. Electrons circulate in bunches in the synchrotron storage ring, generating pulses of far-infrared radiation with a repetition frequency of 52.9 MHz. The Ti:sapphire laser produces pulses with a repetition frequency of 105.8 MHz and a pulse picker selects every other pulse to match the synchrotron pulse pattern. The selected laser pulses are delivered over a fiber optic cable to the sample and the synchrotron pulse probes the photoinduced transmission at a fixed time delay afterward. To synchronize the synchrotron and laser pulses, the 52.9 MHz bunch timing signal from a pair of electrodes inside the synchrotron ring chamber is used by the Synchro-Lock laser control system as a reference for the laser pulse emission. The pulse generator introduces an adjustable delay between the laser and synchrotron pulses. The transmitted far-infrared light is detected by a bolometer detector and recorded on a computer.

a lock-in amplifier. The directly obtained quantity is therefore a differential signal, dS/dt . This signal was detected using a B-doped Si bolometer in combination with the lock-in amplifier. Numerical integration yields the photoinduced transmission $S(t)$, which directly follows the excess quasiparticle density.²⁶

To study the effect of magnetic fields and excess carrier density on the recombination dynamics, we measured the magnetic-field and laser-fluence dependent photoinduced transmission for $\text{Nb}_{0.5}\text{Ti}_{0.5}\text{N}$ and NbN thin films. The samples were fully immersed in superfluid ^4He ($T \leq 2$ K) to minimize heating. At this low temperature, the thermal quasiparticle population is small (compared to the number of broken pairs at high fluence) but not zero. The field was applied parallel to the film surface to avoid the complexity of vortex effects (see Ref. 27). Typical results are shown in Fig. 2, where the photoinduced signal $S(t)$ (excess quasiparticle density) is plotted against delay time. At both low [Figs. 2(a) and 2(c)] and high laser fluences [Figs. 2(b) and 2(d)], a longer time is required for recombination as the magnetic field is increased. The pulse width of the synchrotron probe beam gives rise to the initial upturn in the data, which is skipped in the following data analysis. When the measurements were performed above the superfluid transition, the decay shows a long-lived tail due to the inefficient escape of phonons in the film.

We have discovered a revealing perspective to display our results, shown in Fig. 3. We define an effective instantaneous recombination rate $1/\tau_{\text{eff}}(t) \equiv -[dS(t)/dt]/S(t)$ and plot $1/\tau_{\text{eff}}(t)$ vs $S(t)$ at various fields and fluences. Here short times

are at the right [large $S(t)$] and long times at the left. In this presentation, data at the same field but for different pump fluences scale to the same straight line. As will be shown below, this behavior is expected for bimolecular recombination where the lifetime for a given particle is proportional to the availability of other particles with which to combine.

The scaling can be understood as follows. The phonon bottleneck was first discussed by Rothwarf and Taylor⁴ using two rate equations, one for the quasiparticles and the other for the 2Δ phonons. The quasiparticles, which directly correspond to our signal $S(t)$, follow a simple model that captures the feature of bimolecular recombination, meanwhile taking into account the phonon bottleneck. The decay rate of the total quasiparticle density $N(t)$ toward the equilibrium density is proportional to N^2 , because recombination requires the presence of two quasiparticles. Motivated by the Rothwarf-Taylor⁴ equations, we write

$$\frac{dN}{dt} = -2R(N^2 - N_{\text{th}}^2). \quad (1)$$

A thermal term N_{th}^2 is subtracted from N^2 , because at equilibrium $N = N_{\text{th}}$ and the quasiparticle density must remain constant. The phonon bottleneck is introduced into the model through the recombination rate coefficient R . (See Sec. 1 of the Supplemental Material.³⁸) A factor of 2 is included because each recombination event depletes two quasiparticles. Now, $N(t) = N_{\text{th}} + N_{\text{ex}}(t)$, with N_{th} the thermal density and $N_{\text{ex}}(t)$ the photoinduced excess density. At a given temperature

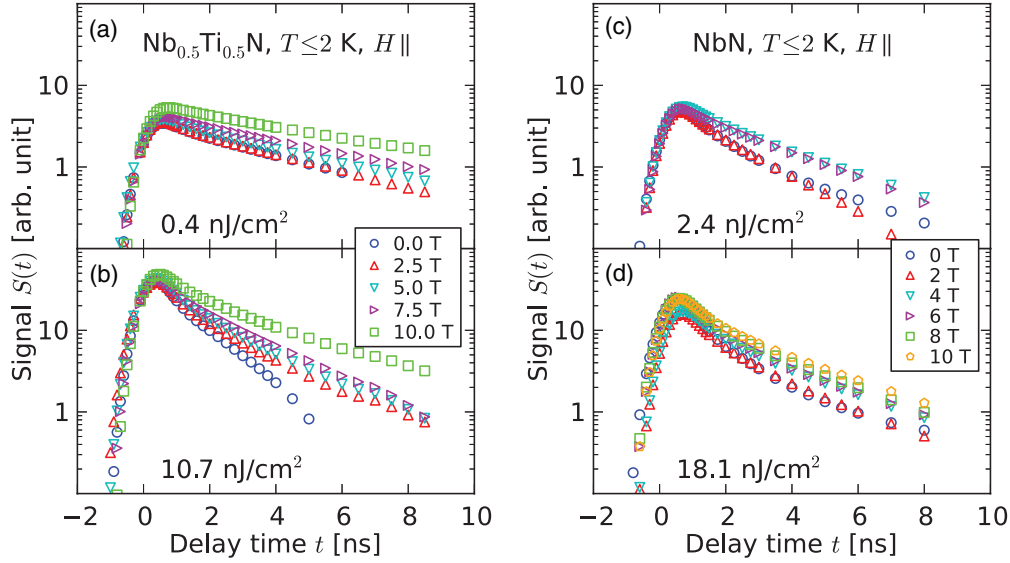


FIG. 2. (Color online) Photoinduced transmission $S(t)$ vs time t for $\text{Nb}_{0.5}\text{Ti}_{0.5}\text{N}$ [(a) and (b)] and for NbN [(c) and (d)], all measured in parallel fields at $T \leq 2$ K. Low-fluence and high-fluence data are compared. Note the semilog scale; simple exponential decay produces a straight line.

and magnetic field, N_{th} is time independent, making Eq. (1) become $-(dN_{\text{ex}}/dt)/N_{\text{ex}} = 2R[N_{\text{ex}}(t) + 2N_{\text{th}}]$. We identify $-(dN_{\text{ex}}/dt)/N_{\text{ex}}$ as the effective instantaneous relaxation rate $1/\tau_{\text{eff}}(t)$ defined earlier, because the photoinduced transmis-

sion $S(t)$ is proportional to the excess quasiparticle density,²⁶ $S = CN_{\text{ex}}$, where C is just a constant to convert from signal to quasiparticle density. Hence,

$$-\frac{1}{S(t)} \frac{dS(t)}{dt} = \frac{2R}{C} [S(t) + 2S_{\text{th}}], \quad (2)$$

with $S_{\text{th}} = CN_{\text{th}}$. Equation (2) is consistent with the linear behavior demonstrated in Fig. 3. The field dependence requires the prefactor R to decrease with field.

To interpret the field dependence shown in Fig. 3, it is a prerequisite to understand how the field changes the electronic states of the superconductor. If spin-orbit scattering is small, the magnetic field could make the majority of quasiparticles have one spin direction. (This is the same polarization that gives Pauli paramagnetism to metals.) Spin polarization will slow the recombination because only quasiparticles with opposite spins can recombine. A recombination model including this spin polarization effect is discussed in Sec. 2 of the Supplemental Material.³⁸ In this case, the recombination equation remains in the same form as Eq. (2), but with the coefficient $2R/C$ replaced by $(8R/C)(N^{\uparrow}N^{\downarrow}/N^2)$, where N^{\uparrow} and N^{\downarrow} are respectively the densities of spin-up and spin-down quasiparticles. The quasiparticle spin-polarization factor $N^{\uparrow}N^{\downarrow}$ would depend on the magnetic field in the limit of weak spin-orbit coupling, just as in the Pauli paramagnetism of metals. According to the BCS theory, electrons form spin-singlet pairs condensed in the ground state; the spin susceptibility vanishes as the temperature approaches 0. The studies of superconductor spin susceptibility were done on thin films with thickness so small that the effect of a magnetic field on the electron orbit could be neglected. Paramagnetic splitting of the quasiparticle density of states was observed in 5 nm aluminum films in a parallel magnetic field.²⁸ In a study of magnetic field effects on far-infrared absorption of thin superconducting aluminum films, van Bentum and Wyder²⁹ concluded that paramagnetic splitting was important

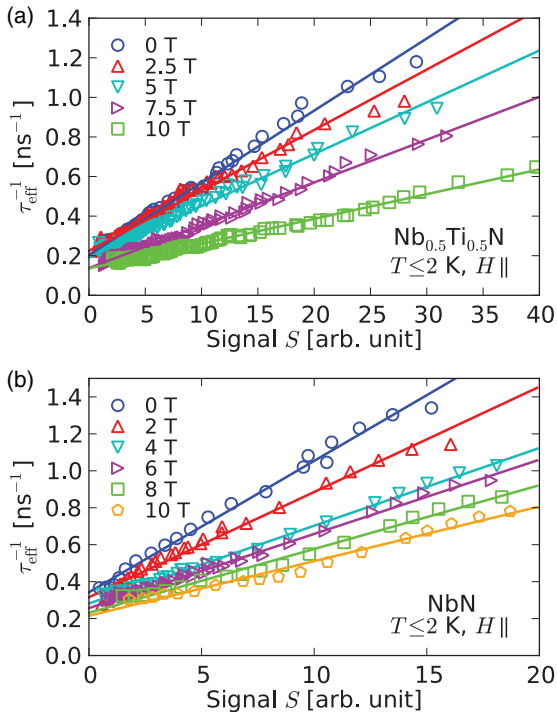


FIG. 3. (Color online) Effective instantaneous recombination rate vs photoinduced transmission. (a) For $\text{Nb}_{0.5}\text{Ti}_{0.5}\text{N}$, data at each field include fluences ranging from 0.4 to 10.7 nJ/cm^2 . (b) For NbN , data at each field include fluences ranging from 2.4 to 18.1 nJ/cm^2 except for 8 T and 10 T, where data were collected at 18.1 nJ/cm^2 . A 4-point moving average was performed on the data to reduce noise. The lines are linear fits to the data.

in their thinnest films, but did not allow for quasiparticle spin polarization. If a high degree of spin polarization existed, the recombination rate would be slowed much more than observed. However, spin-orbit scattering must be considered. Tedrow and Meservey observed the spin-state mixing in thin aluminum films due to spin-orbit scattering.³⁰ They defined a spin-orbit scattering parameter $b \equiv \hbar/3\Delta\tau_{so}$ to describe the degree of spin-orbit scattering, where τ_{so} is the spin-orbit scattering time. They calculated that as b is increased to 0.5, the spin-up and spin-down quasiparticle density of states completely mix, leaving no clear signature of the two-peak feature in the density of states due to Zeeman splitting. Considering the short spin-orbit scattering time measured³¹ in NbTi, $\tau_{so} = 3.0 \times 10^{-14}$ s, and using the Δ of Nb_{0.5}Ti_{0.5}N and NbN, we estimate that $b = 4.2$ and 3.3 for Nb_{0.5}Ti_{0.5}N and NbN, respectively. We believe that spin is not a good quantum number in our samples, requiring us to look beyond spin polarization to understand the recombination.

In a study²⁷ of the optical conductivity of Nb_{0.5}Ti_{0.5}N, we found that a parallel magnetic field breaks the time-reversal symmetry of the Cooper pairs and decreases the superconducting energy gap. The physics is similar to magnetic-impurity-induced pair-breaking effects, as originally formulated by Abrikosov and Gorkov.³² In a magnetic field, one must distinguish between the spectroscopic energy gap $2\Omega_G$ and the pair-correlation gap Δ . These gaps³³ are plotted in Fig. 4(a) as squares and triangles, respectively. The real part of the optical conductivity, corresponding to the electromagnetic absorption, shows a clear suppression of the energy gap $2\Omega_G$ with field [squares in Fig. 4(a)]. The imaginary conductivity is a measure of the superconducting condensate density N_{sc} , which goes as Δ^2 . The field dependencies of Δ and of $\sqrt{N_{sc}}$ (shown as circles) agree well, providing clear evidence for a weakening

of superconductivity by the magnetic field. The quantities Ω_G , Δ , and N_{sc} for NbN, obtained using the same technique (in Sec. 3 of the Supplemental Material³⁸), are plotted in Fig. 4(b). The NbN field dependence is qualitatively different from that of Nb_{0.5}Ti_{0.5}N because in this thicker film the applied field induces a spatial variation in the order parameter, making the weakening of superconductivity be proportional to the field, rather than being quadratic in field as in the much thinner Nb_{0.5}Ti_{0.5}N.³⁴ The energy gaps will be used in the following analysis.

The field dependence, shown in Fig. 3, is dominated by the recombination rate coefficient R . On the one hand, by explicitly solving Eq. (2) one can identify a low-fluence recombination rate $1/\tau_{eff} = 4RN_{th}$. (See Sec. 4 of the Supplemental Material.³⁸) The field dependence of the thermal quasiparticle density N_{th} results from the field-dependent energy gap and the quasiparticle density of states.³⁵ On the other hand, the effective lifetime of the excess quasiparticles is modified from the intrinsic value τ_R , and is tied to the rates at which the phonons, produced in recombination events, rebreak pairs ($1/\tau_B$) or escape from the film ($1/\tau_\gamma$).³⁶ The quasiequilibrium values of τ_R and τ_B were derived by Kaplan *et al.*¹⁵ Magnetic-field-induced pair breaking decreases the spectroscopic energy gap (Fig. 4) and modifies the quasiparticle density of states, resulting in a decrease in τ_R and an increase in τ_B . The field-independent phonon escape time is determined by the film thickness and the acoustic mismatch between the film and the environment.³⁷ The recombination rate coefficient R (and, hence, the slope of $1/\tau_{eff}$ in Fig. 3) is therefore field dependent through N_{th} , τ_R , and τ_B . (See Fig. S7 in the Supplemental Material.³⁸) The equation is involved but, when we compute the slope vs Ω_G for Nb_{0.5}Ti_{0.5}N and NbN, shown in Figs. 4(c) and 4(d), we obtain a basically linear relation. This calculation

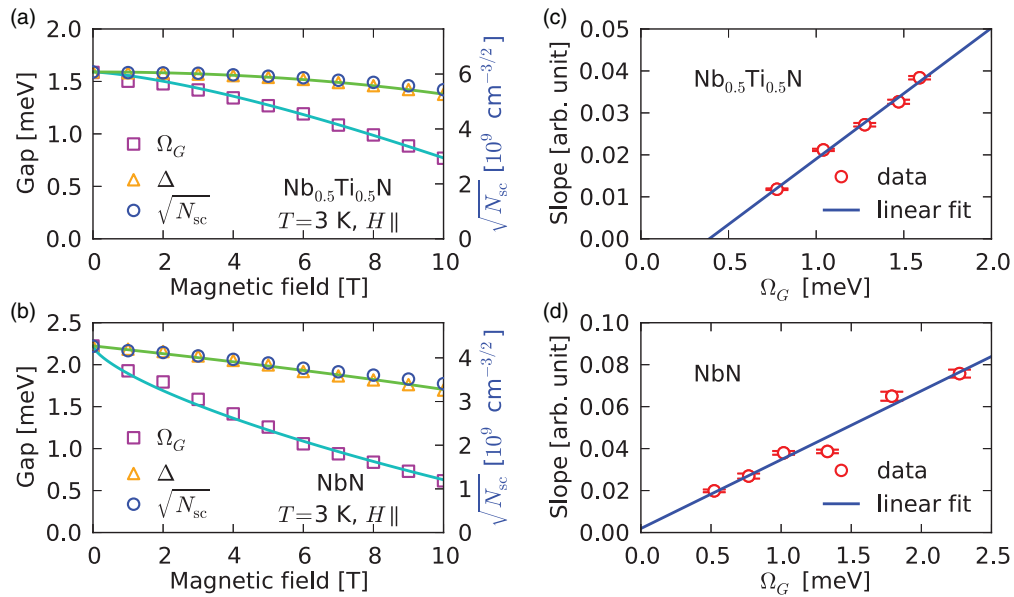


FIG. 4. (Color online) Panels (a) and (b) show the excitation gap Ω_G (squares) and the pair-correlation gap Δ (triangles) for Nb_{0.5}Ti_{0.5}N and NbN, obtained from the optical conductivity (left scale). The solid lines are theoretical calculations of Δ and Ω_G . The square root of the condensate density $\sqrt{N_{sc}}$ (proportional to the order parameter) is shown as circles (right scale). Panels (c) and (d) show the slope extracted from Fig. 3 vs Ω_G from (a) and (b). The error bars in both plots are calculated deviations of the slope from the linear fit in Fig. 3. The lines are linear fits to the circles.

implies a connection between the field-dependent quasiparticle recombination and the field-induced pair breaking. The linear relation can be explained by considering only the field-induced gap reduction. (See Fig. S7 in the Supplemental Material.³⁸) The finite y intercepts in Figs. 4(c) and 4(d) are intriguing, bringing out the question of how the photoexcited quasiparticles relax in a gapless superconductor, motivating challenging experiments to probe the gapless regime.

In conclusion, our time-resolved pump-probe measurements on metallic s -wave superconductors reveal a slowing of quasiparticle recombination in an external magnetic field. The field was aligned parallel to the thin-film sample surface, to minimize effects due to vortices. There are two possible causes of the observed slowing: field-induced spin imbalance and field-induced gap reduction. The spin imbalance is unlikely

to be important in $\text{Nb}_{0.5}\text{Ti}_{0.5}\text{N}$ and NbN due to strong spin-orbit scattering. This scenario can be tested by investigating materials with small spin-orbit scattering. The field-induced gap reduction alone can explain quantitatively the slowing of recombination, and we conclude that it is the dominant effect observed in our experiment.

We thank P. Bosland and E. Jacques for providing the samples, J. J. Tu for access to the magnet, R. P. S. M. Lobo for data acquisition software development, G. Nintzel and R. Smith for technical assistance, and P. J. Hirschfeld for discussions. This work was supported by the US Department of Energy through Contracts No. DE-ACO2-98CH10886 (Brookhaven National Laboratory) and No. DEFG02-02ER45984 (University of Florida), and by the National Research Foundation of Korea through Grant No. 20100008552.

-
- ¹D. M. Ginsberg, *Phys. Rev. Lett.* **8**, 204 (1962).
²J. R. Schrieffer and D. M. Ginsberg, *Phys. Rev. Lett.* **8**, 207 (1962).
³L. Tewordt, *Phys. Rev.* **127**, 371 (1962).
⁴A. Rothwarf and N. Taylor, *Phys. Rev. Lett.* **19**, 27 (1967).
⁵I. Schuller and K. E. Gray, *Phys. Rev. B* **12**, 2629 (1975).
⁶C. C. Chi, M. M. T. Loy, and D. C. Cronmeyer, *Phys. Rev. B* **23**, 124 (1981).
⁷J. F. Federici, B. I. Greene, P. N. Saeta, D. R. Dykaar, F. Sharifi, and R. C. Dynes, *Phys. Rev. B* **46**, 11153 (1992).
⁸G. L. Carr, R. P. S. M. Lobo, J. LaVeigne, D. H. Reitze, and D. B. Tanner, *Phys. Rev. Lett.* **85**, 3001 (2000).
⁹J. Demsar, R. D. Averitt, A. J. Taylor, V. V. Kabanov, W. N. Kang, H. J. Kim, E. M. Choi, and S. I. Lee, *Phys. Rev. Lett.* **91**, 267002 (2003).
¹⁰M. Beck, M. Klammer, S. Lang, P. Leiderer, V. V. Kabanov, G. N. Goltsman, and J. Demsar, *Phys. Rev. Lett.* **107**, 177007 (2011).
¹¹N. Gedik, P. Blake, R. C. Spitzer, J. Orenstein, Ruixing Liang, D. A. Bonn, and W. N. Hardy, *Phys. Rev. B* **70**, 014504 (2004).
¹²P. Kusar, V. V. Kabanov, J. Demsar, T. Mertelj, S. Sugai, and D. Mihailovic, *Phys. Rev. Lett.* **101**, 227001 (2008).
¹³T. Mertelj, V. V. Kabanov, C. Gadermaier, N. D. Zhigadlo, S. Katrych, J. Karpinski, and D. Mihailovic, *Phys. Rev. Lett.* **102**, 117002 (2009).
¹⁴D. Mihailovic and J. Demsar, *Spectroscopy of Superconducting Materials* (American Chemical Society, Washington, DC, 1999), pp. 230–244.
¹⁵S. B. Kaplan, C. C. Chi, D. N. Langenberg, J. J. Chang, S. Jafarey, and D. J. Scalapino, *Phys. Rev. B* **14**, 4854 (1976).
¹⁶J. J. Chang and D. J. Scalapino, *Phys. Rev. B* **15**, 2651 (1977).
¹⁷J. L. Levine and S. Y. Hsieh, *Phys. Rev. Lett.* **20**, 994 (1968).
¹⁸N. Perrin, *Phys. Lett. A* **90**, 67 (1982).
¹⁹P. Fulde, *Mod. Phys. Lett. B* **24**, 2601 (2010).
²⁰K. Holdik, M. Welte, and W. Einsenmenger, *J. Low Temp. Phys.* **58**, 379 (1985).
²¹F. Hübler, J. Camirand Lemyre, D. Beckmann, and H. v. Löhneysen, *Phys. Rev. B* **81**, 184524 (2010).
²²F. Hübler, M. J. Wolf, D. Beckmann, and H. v. Löhneysen, *Phys. Rev. Lett.* **109**, 207001 (2012).
²³C. H. L. Quay, D. Chevallier, C. Bena, and M. Aprili, *Nat. Phys.* **9**, 84 (2013).
²⁴A. V. Timofeev, C. Pascual García, N. B. Kopnin, A. M. Savin, M. Meschke, F. Giazotto, and J. P. Pekola, *Phys. Rev. Lett.* **102**, 017003 (2009).
²⁵K. Yu. Arutyunov, H.-P. Auraneva, and A. S. Vasenko, *Phys. Rev. B* **83**, 104509 (2011).
²⁶R. P. S. M. Lobo, J. D. LaVeigne, D. H. Reitze, D. B. Tanner, Z. H. Barber, E. Jacques, P. Bosland, M. J. Burns, and G. L. Carr, *Phys. Rev. B* **72**, 024510 (2005).
²⁷X. Xi, J. Hwang, C. Martin, D. B. Tanner, and G. L. Carr, *Phys. Rev. Lett.* **105**, 257006 (2010).
²⁸R. Meservey, P. M. Tedrow, and P. Fulde, *Phys. Rev. Lett.* **25**, 1270 (1970).
²⁹P. J. M. van Bentum and P. Wyder, *Phys. Rev. B* **34**, 1582 (1986).
³⁰P. M. Tedrow and R. Meservey, *Phys. Rev. Lett.* **27**, 919 (1971).
³¹R. R. Hake, *Appl. Phys. Lett.* **10**, 189 (1967).
³²A. A. Abrikosov and L. P. Gor'kov, *Sov. Phys. JETP* **12**, 1243 (1961).
³³S. Skalski, O. Betbeder-Matibet, and P. R. Weiss, *Phys. Rev.* **136**, A1500 (1964).
³⁴R. D. Parks, *Superconductivity* (Marcel Dekker, New York, 1969).
³⁵R. Bayrle and O. Weis, *J. Low Temp. Phys.* **76**, 143 (1978).
³⁶K. E. Gray, *J. Phys. F: Met. Phys.* **1**, 290 (1971).
³⁷J. J. Chang and D. J. Scalapino, *J. Low Temp. Phys.* **31**, 1 (1978).
³⁸See Supplemental Material at <http://link.aps.org/supplemental/10.1103/PhysRevB.87.140502> for more details.